Partially Cavitating Cascades

In the context of pumps, the solutions by Acosta and Hollander (1959) and Stripling and Acosta (1962) of partial cavitation in a semi-infinite cascade of infinitely thin blades and the solution by Wade (1967) of a finite cascade of partially cavitating foils provide a particularly valuable means of analyzing the performance of two-dimensional cascades with blade cavities. More recently the three dimensional aspects of these solutions have been explored by Furuya (1974). As a complement to purely analytical methods, more heuristic approaches are possible in which the conventional cascade analyses (see sections (Mbcb), (Mbce)) are supplemented by lift and drag data for blades operating under cavitating conditions.
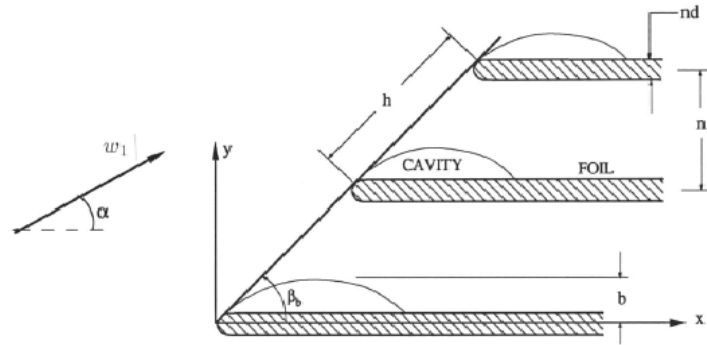

Figure 1: Schematic of partially cavitating cascade of flat blades of thickness nd (Brennen and Acosta 1973).

Partly for the purposes of example and partly because the results are useful, we shall recount here the results of the free-streamline solution of Brennen and Acosta (1973). This is a slightly modified version of the Acosta and Hollander solution for partial cavitation in a cascade of infinitely thin, flat blades. The modification was to add finite thickness to the blades. As we shall see, this can be important in terms of the relevance of the theory.

A sketch of the cascade geometry is shown in figure 1. A single parameter is introduced to the solution in order to yield finite blade thickness. This parameter implies a ratio, d, of the blade thickness far downstream to the normal spacing between the blades. It also implies a radius of curvature of the parabolic leading edge of the blade, κ, given by

$$\frac{1}{\kappa} \approx \frac{d^2 \beta_b^3}{\pi h (1 + \sigma_c)} \tag{Mbeu1}$$

where σ_c is the choked cavitation number (see below). Equation (Mbeu1) and the fact that the ultimate thickness is not reached until about half a blade spacing downstream, both imply very sharp leading edges.

One of the common features of all of these free streamline solutions is that there exists a certain minimum cavitation number at which the cavity becomes infinitely long and below which there are no solutions. This minimum cavitation number is called the choked cavitation number, σ_c. Were such a flow to occur in practice, it would permit large deviation angles at discharge and a major degradation of performance. Consequently the choked cavitation number, σ_c, is often considered an approximation to the breakdown cavitation number, σ_b, for the pump flow which the cascade solution represents. The Brennen and Acosta solution yields a choked cavitation number given by

$$\sigma_c = \left[1 + 2 \sin \frac{\alpha}{2} \sec \frac{\beta_b}{2} \sin \frac{(\beta_b - \alpha)}{2} + 2d \sin^2 \frac{\beta_b}{2} \right]^2 - 1 \tag{Mbeu2}$$

which, since the solution is only valid for small incidence angles, α, and since β_b is normally small, yields

$$\sigma_c \approx \alpha(\beta_b - \alpha) + \beta_b^2 d \qquad \text{(Mbeu3)}$$

Furthermore, at a general cavitation number, σ, the maximum thickness, b, of the cavity is given by

$$\frac{b}{n} = 2\pi \left[d - (1 + \sigma)^{\frac{1}{2}} + \sin(\beta_b - \alpha)/\sin \beta_b \right] \qquad \text{(Mbeu4)}$$

or

$$\frac{b}{n} \approx 2\pi \left[d - \frac{\alpha}{\beta_b} - \frac{\sigma}{2} \right] \qquad \text{(Mbeu5)}$$

As a rough example, consider a $10°$ helical inducer ($\beta_b = 10°$) with a fractional blade thickness of $d = 0.15$ operating at a flow coefficient, $\phi = 0.08$, so that the incidence angle, $\alpha = 4°$ (see figure 5). Then, according to the relation (Mbeu3), the choked cavitation number is $\sigma_c = 0.0119$ which is close to the observed breakdown cavitation number (see figure 7). It is important to note the role played by the blade thickness in this typical calculation because with $d = 0$ the result is $\sigma_c = 0.0073$. Note also that with infinitely thin blades, the expression (Mbeu3) predicts $\sigma_c = 0$ at zero incidence. Thus, the blade thickness is important in estimating the choked cavitation number in any pump.
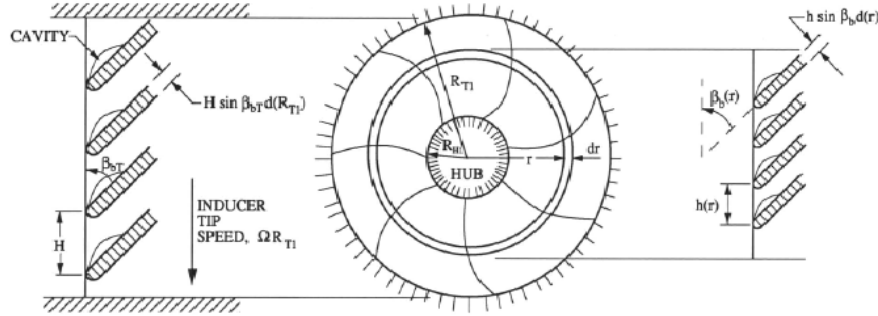

Figure 2: The subdivision of the flow through an axial inducer into radial annuli for cascade analysis.

Most pumps or inducer designs incorporate significant variations in α, β_b and d over the inlet plane and hence the above analysis has to be performed as a function of the inlet radial position as indicated in figure 2. Typical input data for such calculations are shown in figures 3, 5 and 6 for the Saturn J2 and F1 liquid oxygen turbopumps, for the $9°$ helical inducer, Impeller III, and for the SSME low pressure liquid oxygen impeller, Impeller IV. To proceed with an evaluation of the flow, the cascade at each radial annulus must then be analyzed in terms of the cavitation number, $\sigma(r)$, pertaining to that particular radius, namely

$$\sigma(r) = (p_1 - p_V)/\frac{1}{2}\rho_L \Omega^2 r^2 \qquad \text{(Mbeu6)}$$

Specific values of this cavitation number at which choking occurs in each cascade can then be obtained from equations (Mbeu2) or (Mbeu3); we denote these by $\sigma_c(r)$. It follows that the *overall* pump cavitation number at which the flow in each annulus will be choked is given by $\sigma_{cT}(r)$ where

$$\sigma_{cT}(r) = \sigma_c(r) r^2 / R_{T1}^2 \qquad \text{(Mbeu7)}$$

Typical data for $\sigma_{cT}(r)$ for the Saturn J2 and F1 oxidizer pumps are plotted in figure 4; additional examples for Impellers III and IV are shown in figure 7. Note that, in theory, the flow at one particular radial location will become choked before that at any other radius. The particular location will depend on the radial distributions of blade angle and blade thickness and may occur near the hub (as in the cases
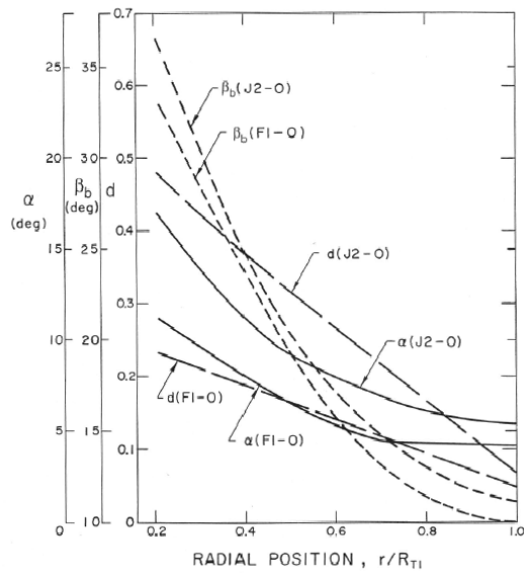
Figure 3: Radial variations of the blade angle, β_b, blade thickness to normal spacing ratio, d, and incidence angle α (for $\phi = 0.097$) for the oxidizer turbopumps in the Saturn J1 and F1 engines (from Brennen and Acosta 1973).
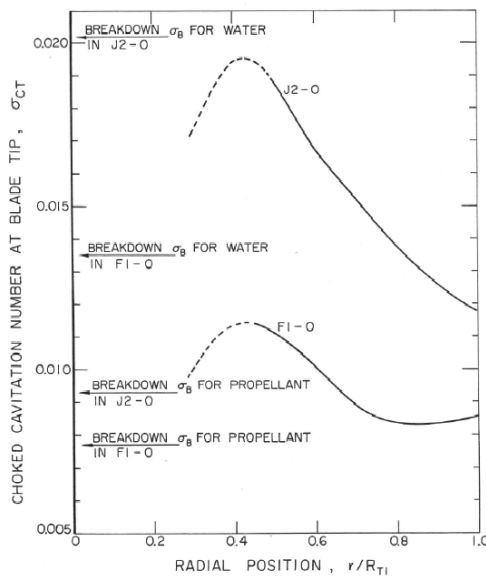

Figure 4: The tip cavitation numbers at which the flow at each radial location becomes choked. Data is shown for the Saturn J2 and F1 oxidizer turbopumps (see figure 3); experimentally observed breakdown cavitation numbers in water and propellant are also shown (from Brennen and Acosta 1973).

shown in figure 4) or near the tip. However, one might heuristically argue that once the flow at any radius becomes choked, the flow through the pump will reach breakdown. On this basis, the data of figure 4 would predict breakdown in the J2-O turbopump at $\sigma_b \approx 0.019$ and at 0.0125 for the F1-O turbopump. In table 1 and figure 4 these predictions are compared with the observed values from tests in which water is used. The agreement appears quite satisfactory. Some data obtained from tests with propellant rather than water is also shown in figure 4 and exhibits less satisfactory agreement; this is probably the result of thermal effects in the propellant which are not present in the water tests. Moreover, as expected, the predicted results do change with flow coefficient (since this alters the angle of incidence) as illustrated in figure 7.
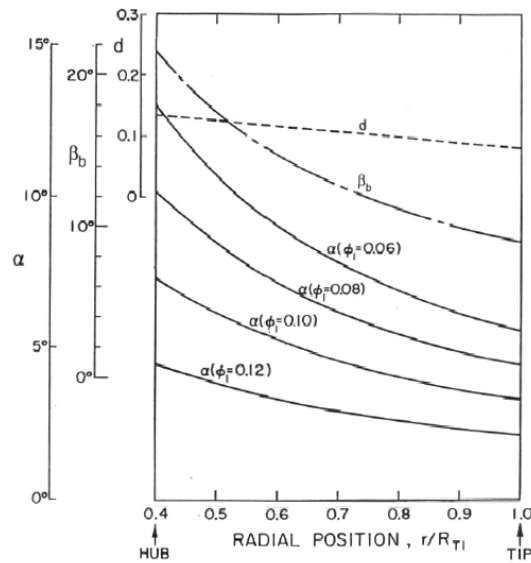
Figure 5: Radial variations of the blade angle, β_b, blade thickness to normal spacing ratio, d, and incidence angle, α, for the $9°$ helical inducer, Impeller III (from Brennen and Acosta 1976).
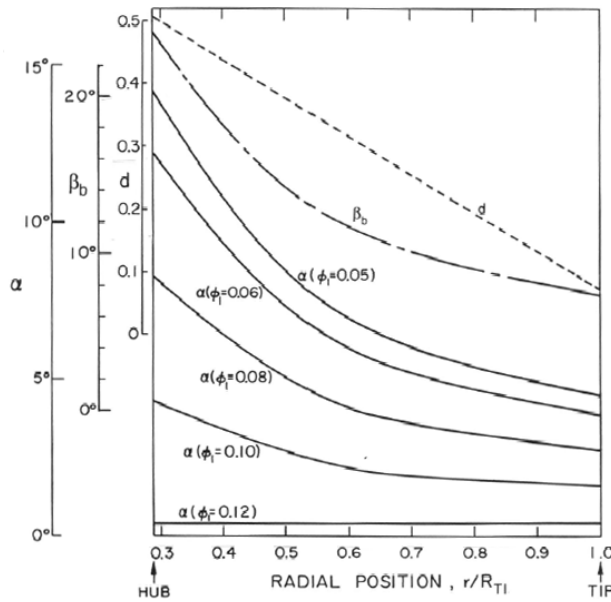

Figure 6: Radial variations of the blade angle, β_b, blade thickness to normal spacing ratio, d, and incidence angle, α, at inlet to the SSME low pressure liquid oxygen pump, Impeller IV (from Brennen and Acosta 1976).

Perhaps the most exhaustive experimental investigation of breakdown cavitation numbers for inducers is the series of experiments reported by Stripling (1962) in which inducers with blade angles at the tip, β_{bT1}, varying from $5.6°$ to $18°$, various leading edge geometries, blade numbers of 3 and 4 and two hub-to-tip ratios were investigated. Some of Stripling's experimental data is presented in figure 8 where the σ_b values are plotted against the flow coefficient, ϕ_1. In his paper Stripling argues that the data correlate with the parameter $\phi_1 \sin\beta_{bT1}/(1 + \cos\beta_{bT1})$ but, in fact, the experimental data are much better correlated with ϕ_1 alone as demonstrated in figure 8. There is no satisfactory explanation for the fact that σ_b correlates better with ϕ_1.

Stripling correlates his data with the theoretical values of the choked cavitation number which one would obtain from the above theory in the case of infinitely thin blades. (In this limit the expression
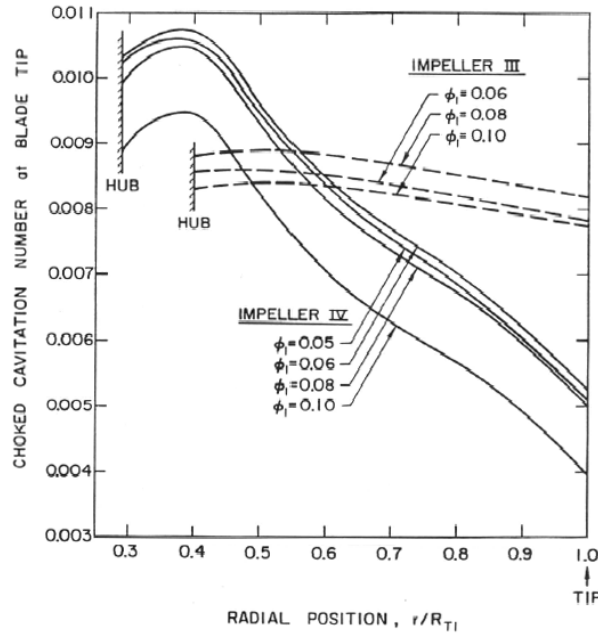
Figure 7: The tip cavitation numbers at which the flow at each radial location becomes choked for Impellers III and IV (see figures 5 and 6) and different flow coefficients, ϕ_1 (from Brennen and Acosta 1976).

Table 1: Theoretical predictions of breakdown cavitation numbers compared with those observed during water tests with various inducer pumps.

Inducer	Theory σ_c	Observed σ_b
Saturn J2 Oxidizer Inducer	0.019	0.020
Saturn F1 Oxidizer Inducer	0.012	0.013
SSME Low Pressure LOX Pump	0.011	0.012
9° Helical Impeller III	0.009	0.012

for σ_c is more easily obtained by simultaneous solution of the Bernoulli equation and an equation for the momentum parallel with the blades as Stripling demonstrates.) More specifically, Stripling uses the blade angles, β_{b1}, and incidence angles at the rms radius, R_{RMS}, where

$$ R_{RMS} = \left[\frac{1}{2} \left(R_{T1}^2 + R_{H1}^2 \right) \right]^{\frac{1}{2}} \tag{Mbeu8} $$

His theoretical results then correspond to the dashed lines in figure 8. When the blade thickness term is added as in equation (Mbeu3) the choked cavitation numbers are given by the solid lines in figure 8 which are considerably closer to the experimental values of σ_b than the dashed lines. The remaining discrepancy could well be due to the fact that the σ_c values are larger at some radius other than R_{RMS} and hence breakdown occurs first at that other radius.

Up to this point we have only discussed the calculation of the choked or breakdown cavitation number from the analysis of a partially cavitating cascade. There remains the issue of how to predict the degradation in the head or the cavitation head losses prior to breakdown. The problem here is that calculation of the lift from these analyses produces little for, as one could anticipate, a small partial cavity will not significantly alter the performance of a cascade of higher solidity since the discharge, with or without the cavity, is essentially constrained to follow the direction of the blades. The hydraulic losses which one seeks are additional (or possibly negative) frictional losses generated by the disruption to the flow caused by the cavitation. A number of authors, including Stripling and Acosta (1962), have employed modifications to
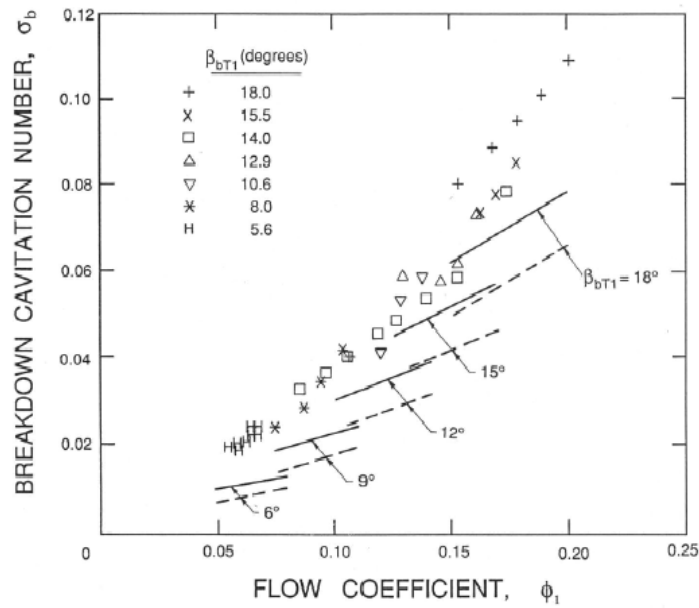
Figure 8: The breakdown cavitation numbers for a series of inducers by Stripling (1962) plotted against inlet flow coefficient. The inducers have inlet blade angles at the tip, β_{bT1} (in degrees), as indicated. Also shown are the results of the cascade analysis (equation (Mbeu3)) applied at the rms radius, R_{RMS}, with blade thickness (solid line) and without blade thickness (dashed line).

cascade analyses in order to evaluate the loss of head, ΔH, due to cavitation. One way to view this loss is to recognize that the presence of a cavity in the blade passage causes a reduction in the cross-sectional area available to the liquid flow. When the cavity collapses this area increases creating a "diffuser" which is not otherwise present. Hydraulic losses in this "diffuser" flow could be considered responsible for the cavitation head loss and could be derived from knowledge of the cavity blockage, b/n.